5/26/95

Large Amplitude IMF Fluctuations in Corotating Interaction Regions: Ulysses at Midlatitudes

Bruce T. Tsurutani
Christian M. Ho
John K. Arballo
Bruce E. Goldstein

Jet Propulsion Laboratory
California Institute of Technology
4800 Oak Grove Drive
Pasadena, CA 91100 USA

Andre Balogh
Imperial College of Science & Technology
The Blackett Laboratory
Prince Consort Road
London SW7 2BZ England

Submitted to Geophysical Research Letters

May 30, 1995

Abstract

Corotating Interaction Regions (CIRs), formed by a high-speed corotating stream interacting with a slow speed stream, have been examined from -20° to -36° heliolatitudes. The high-speed stream emanates from a polar coronal hole that Ulysses eventually becomes fully embedded in as it travels towards south pole. We find that the trailing portion of the CIR, from the interface surface (IF) to the reverse shock (RS), contains both large amplitude transverse fluctuations and magnitude fluctuations. The normalized magnetic field component variances within this portion of the CIR and in the trailing high-speed stream are approximately the same, indicating that the fluctuations in the CIR are compressed Alfvén waves. Mirror mode structures with lower intensities are also observed in the trailing portion of the CIR, presumably generated from a local instability driven by free energy associated with (reverse) shock compression of the high-speed solar wind plasma. The mixture of these two modes (compressed Alfvén waves and mirror modes) plus other modes generated by three wave processes (wave-shock interactions) lead to a lower Alfvénicity within the trailing portion of the CIR than in the high-speed stream proper.

ntroduction

One of he most significant features in the U lysses igh lati ude pass 80°, September 994), was the presence of a continuous high-speed ~750-800 km s^{-1} stream emanating from a polar corona hole (Phillips et al. 994). The stream was also detected at midlatitude (2)° to -36°), where the interaction with a slower, -400 km s^{-1} speed st eam led to the fo mation of corotating interaction regions (CIRs Smith and Wolfe, 1976). The CIRs are often bounded by forward and everse shocks and appeared a 26 da y intervals in ie Ulysses post-Jovian encounter data.

One dominant interplanetary magnetic field (IMF) characteristic of the polar coronal hole stream is the presence of embedded large-amplitude ($\Delta\vec{B}/|B| \sim 1$ to 2) Alfvén waves propaga ing away from the Sun (Tsurutani et al., 1994, 1995; Balogh et al. 1995; Smith et al., 995). The transverse Alfvén waves have been found to be continuous and o fill the entire stream. This recently acquired knowledge of he relationshi bet n Alfvén waves and high-speed streams has led us to consider the interaction depicted in igure 1 The region betwee the stream-stream interface (IF) and the reverse shock (RS) is shocked high-speed stream plasma and fields. Thus, one could expect to detect amplified Alfvén waves in this region due to th ei compression as they are overtaken by the reverse shock. Wave-shock interactions are also expected to occur in this region of space, so other wave modes could be present as wel

The purpose of this paper is to make a preliminary examination of the magnetic field properties in the trailing portions of CIRs to determine the ypes of wave modes presen here and o determine if the hypothetical model of Figure 1 is correct or not. The importance of this is not only from the viewpoint of plasma wave physics, bu i also has implications for geomagnetic activity at arth as wel . Tsurutani et al. (1995) have recently shown that IMF B_z fluctuations within CIRs cause moderate-to-weak geomagnetic storms during the descending phase of the solar cycle. The southward components of hese fluctuations, through magnetic reconnection with the Earth's magnetic fields, cause solar wind energy transfer to the magnetosphere and the magnetic storms. What is presently unknown is the source of the B_z fluctuations.

RESULTS

Figure 1 is a schematic of a stream-stream interaction process projected onto the ecliptic plane (looking down from the north pole). The slow (~400 km s^{-1}) speed stream (A) is on the left and the fast (~750 km s^{-1}) stream (B) is on the right. The interaction region is shaded and is bound by a fast shock (FS) and a reverse shock (RS). The accelerated and compressed slow speed stream is on the antisunward side of the CIR. The decelerated and compressed high speed stream is on the sunward side of the CIR. The two regions are separated by a stream interface (IF). In the high speed stream proper (B), large amplitude transverse Alfvén waves are present (indicated schematically). We expect the presence of compressed Alfvén waves in the trailing portion of the CIR, between the IF and the RS. The waves should be amplified in proportion to the magnitude of the magnetic field jump across the reverse shock. This Figure is only a model which can be tested by the Ulysses observations, which will be discussed below.

We have examined all of the CIRs in the Ulysses post-Jovian encounter data. These CIRs span a latitude range from - 20° to - 36°. There are 10 distinct CIRs in all. Beyond this latitude, Ulysses becomes permanently embedded in the high-speed stream. In Figure 2, we show one typical example. This event occurred when Ulysses was at -36° latitude and 4.5 AU from the Sun. This particular event was the last clear appearance of the CIR.

The RS and IF discontinuities are indicated at the top of Figure 2 by dashed vertical lines. There is not a shock (FS) at the antisolar edge of the CIR, but there are both density and magnetic field compressions at this discontinuity surface. From top to bottom are the field magnitude, solar wind speed, proton density, and temperature. The IF is clearly indicated by sharp increase in the proton density and temperature. The magnetic field magnitude decreases across this boundary as well. The region of interest is the trailing part of the CIR, from the IF to the RS (shaded). There are large |B| fluctuations apparent in the Figure. This will be discussed later.

Figure 3 shows the three components of $\vec{B}$ and $\vec{V}_{SW}$ in solar heliospheric coordinates (RTN), as well as |B| for reference. In this system $\hat{R}$ points outward from the Sun, $\hat{T} = \hat{W} \times \hat{R}/|\hat{W} \times \hat{R}|$, when $\hat{W}$ is the solar rotation axis, and $\hat{N}$ forms a right-hand system. In the region between the IF and the RS, there are large fluctuations in the field components as indicated by the 6 component panels. Although there are fluctuations in |B| as well, the component fluctuations are generally larger. The sum of the three $\vec{B}$ com ponent 20-min variances is shown in the next to bottom panel. It can be noted that these large variances are presentprimarily in this fast stream

compression region. There is a general absence of fluctuations in the region between the first discontinuity and the IF, consistent with the schematic of Figure 1.

One of the most common tests for the Alfvénicity of field fluctuations is the correlation between solar wind velocity and $\vec{B}$. High correlation coefficients at zero lag have been used to indicate of the Alfvénic nature of the fluctuations (Belcher and Davis, 1971), and the sign of the correlation coefficient for the direction of propagation. The results of the cross correlation analyses of the V and $\vec{B}$ components are indicated by lhc:,ray-scale plots at the top of Figure 3. Correlation coefficients for all three S11 components are indicated, with the darkest shading corresponding to a ±1.() correlation at zero lag ∓ 20 min., and whi te corresponding to zero correlation. The correlations were calculated over 4-hour intervals. Note the high level of Alfvén fluctuations in the post-RS (high-speed stream) region. By examining the gray scale results at the top, we find that this region has the highest Alfvénicity (highest correlation coefficients -().8). These waves are propagating outward from the Sun (not shown), even at these. large distances (4.5 AU). The Alfvénicity of the region between the IF and RS is, however, less than the high-sped stream proper. The correlation coefficients are typically -0.4- 0.6.

The magnetic field strength within the CIR is larger than either the Iligh-speed stream proper or the unshocked slow sped stream. 'I'bus, to compare wave amplitudes in different regions of the interplanetary medium, normalization is necessary. 'I 'he variances have been normalized by dividing by $|B|^2$ and the results are shown in Figure 4. The normalized 20-min. variance SH components are given in the top three panels. These values can be used to compare the relative wave power Within the CIR to those ill the high-speed stream proper. Longer duration variances have been examined, and similar results have been obtained.

Figure 4 shows the normalized variances for the event in Figure 3. Plotted in this fashion, it is now noted that the normalized variances within the hig h-speed stream proper (beyond the RS) are comparable to the. normalized variances within the (:11<. "1'bus, it appears that the transverse fluctuations within the trailing portion of the CIR is consistent with being compressed (amplified) Alfvénic turbulence.

'1'here is a local peak in normalized variances at an(l near the reverse shock. This is most easily noted in the $\sigma_N^2/|B|^2$ and $\sigma_T^2/|B|^2$ panels. This additional power cannot be due to shock compression alone.

The insert of Figure 4 shows the field magnitude in higher time resolution. Also superposed on this are results from minimum variance analyses of individual wave cycles present in the data. 11 is generally found that close to the RS, the waves are propagating at large, angles relative to the ambient magnetic field (~50° - 90<'). This is in sharp contrast with Alfvén waves in the high-speed stream J) I"[J)Cl", for which angles of propagation are typically 0° - 2 0[' relative to $\vec{B}$ (not shown).

Figure **5a is** high resolution magnetic field data from 1650 to J 706 UT day 206, 1994. Note that there are many small |B I decreases in the interva 1. All of these. decreases are not associated with any notice.able field angular changes. This characteristic has been previously used to identify mirror mode structures in the magnetosheaths of Earth, Jupiter and Saturn (Tsurutani et al., 1982; 1993). Wc have examined the instability criteria for mirror mode growth, $R = (\beta_\perp/\beta_{||})/(1 + 1/\beta_\perp)$. In this expression $\beta = 8\pi nkT/B^2$, and the subscripts $\perp$ and || indicate that values are taken perpendicular and parallel values with respect to the ambient magnetic field. This is shown in the insert of Figure 4. For the interval given, R is ~0.8. Growth occurs at $R > 1.0$, thus the structures shown arc Stable.

The entire IF to RS inter-va] has been examined for mirror instability/stability, and we find that there is only one clear region of positive mirror mode growth. This is near the reverse shock. '1'here R is -1.5. '1'bus, one. scenario is that the source of free energy for mirror mode growth is (reverse) shock compression of the high-speed protons. once mirror structures begin to form, they decrease the free energy (proton anisotropy) available, and bring the remainder of the trailing portion of the. CIR to marginal stability (R = 0.5 to 1 .()).

Panel 5b is the. hodogram of the wave shown in panel a. The interval is 1700:51 to 1704:49 UT, day 206. This wave is just adjacent (but dots not overlap) with the mirror mode structure at 1700:00 UT. The field is shown in minimum variance coordinates, where B_1, B_2, B_3 correspond to the field in the maximum, intermediate and minimum variance directions (Smith and Tsurutani, 1976). In this example, the $\vec{B}$ is out of the plane. Thus the wave is left-hand elliptically polarized, ($\lambda_1/\lambda_2 = 4.7$, $\lambda_2/\lambda_3 = 1.2$). The angle of propagation is 13° dative to $\vec{B}$.

SUMMARY

Wc find that there are both large field component and magnitude fluctuations within the trailing half of CIRs, from the IF to the 1<S. This is in distinct contrast to the leading half of CIRs. From

$V - \vec{B}$ correlation analyses, we find that this former region is less Alfvénic than in the high-sped stream proper.

Alfvén wave propagation directions within the trailing portion of the CIR have been found to be significantly more oblique (50" - 90°) than in the. high-speed stream proper. Onc wave case has been shown to be left-hand elliptical] y polarized in the spacecraft frame. However typical wave cases have linear or arc-polarization.

The variance analyses have shown that the normalized component fluctuations are the same both inside and outside the CIR, giving strong weight to the possibility that the transverse fluctuations within the trailing portions of CIRs arc simply shock amplified Alfvén waves.

Large variances near the RS also indicate that wave-wave interactions or wave generation are possibly occurring at and near the shock. However, the lack of high resolution plasma data precludes a detailed analysis of potential wave modes at this time.

Another mode that appears to be locally generated at and near the RS is mirror mode structures. 'his occurs due to the compression of the high-speed stream plasma, creating the necessary plasma anisotropies which lead to local growth of the mode (R = 1.5). These structures are primarily compressive and have little or no field angular changes associated with them.

in conclusion, wc find that the normalized variance results arc consistent with the hypothesis that much of the magnetic field component fluctuations in the trailing portion of the CIR are Alfvénic. The direction of the Alfvén wave propagation appears to be altered, perhaps through refraction as the wave propagates into the high density CIR structure. However, other modes, such as the mirror, arc present as well. Alfvén wave-sl)ock interactions may produce even more modes in addition to the two discussed above. l'bus, the lack of strong Alfvénicity within the trailing portion of CIRs is due to the presence of two or more wave modes intermixed with each other,

Acknowledgments: Portions of this work were performed at the Jet Propulsion Laboratory, California Institute of Technology, Pasadena, under contract with the National Aeronautics and Space Administration.

References

Balogh, A., E. J, Smith, B. T. Tsurutani, D. J. Southwood, R. J. Forsyth, and T. S. Hornbury, The heliospheric magnetic field over south polar regions of the Sun, to appear in Science, 1995.

Phillips, J. L., A. Balogh, S. J. Bame, B. E. Goldstein, J. T. Gosling, J. T. Hoeksema, D. J. McComas, M. Neugebauer, N. R. Sheeley, Jr., and Y. M. Yang, Ulysses at 50" south, Constant immersion in the high-speed solar wind, Geophys. Res. Lett., 21, **1105,** 1994.

Smith, E. J. and B. T. Tsurutani, Magnetosheath lion roars, J. Geophys Res., 81, 2261, 1976.

Smith, E. J. and J. H., Wolfe, observations of interaction regions and corotating shocks between one and five AU: Pioneers 10 and 11, Geophys. Res. Lett., 3, 137, 1976.

Smith, E. J., A. Balogh, R. P. Lepping, M. Neugebauer, J. Phillips and B. "1'. Tsurutani, Ulysses observations of latitude gradients in the heliospheric magnetic field, Ad. Space Res., 16, 165, 1995.

Tsurutani, B. T., E. J. Smith, R. R. Anderson, K. W. Ogilvie, J. D. Scudder, D. N. Baker, and S. J. Bame, Lion roars and nonoscillatory drift mirror waves in the magnetosheath, J. Geophys. Res., 87, 6060, 1982.

Tsurutani, B. 'F'., D. J. Southwood, E. J. Smith and A. Balogh, A survey of low frequency waves at Jupiter: The Ulysses encounter, J. Geophys. Res., 98, 21 203, 1993.

Tsurutani, B. T., C. M. Ho, E. J. Smith, M. Neugebauer, B. E. Goldstein, J. S. Mok, J. K. Arballo, A. Balogh, D. J. Southwood and W. C. Feldman, The relationship between interplanetary discontinuities and Alfvén waves: Ulysses observations, Geophys. Res. Lett., 21, 2267, 1994.

Tsurutani, B. T., E. J. Smith, C. M. Ho, M. Neugebauer, B. F. Goldstein, J. S. Mok, A. Balogh, D. Southwood and W. C. Feldman, Interplanetary discontinuities and Alfvén waves, Space Sci. Rev., 72, **205, 1995.**

Figure Captions

Figure 1. The **interaction** of a high-speed stream (B) with a slow speed stream (A) and the corotating interaction region (CIR) formed (shaded). The forward shock (FS), interface surface (IF). and reverse shock (RS) are indicated. The Alfvén waves present in the high-speed stream proper (B) will be compressed as they are swept up by the expanding reverse shock. Such amplified waves will be found in the CIR between the IF and RS.

Figure 2. A CIR at -36" latitude and 4.5 AU from the Sun. The three boundaries within the CIR are indicate.d by vertical dashed lines. The region of interest, from the interface (IF) to the reverse shock (RS) is shaded.

Figure 3. The same CIR as in Figure 2, but with the magnetic field and velocity components shown. The very large field component fluctuations are quantitatively indicated by the large variances (σ_2), generally the largest within the interval shown. The top panel shows the $\vec{V} - \vec{B}$ component correlation coefficients. The high-speed stream region (10 UT, day 207 and beyond) is highly Alfvénic (c.c. > 0.8), whereas the region between the 1 t'and RS is far less so.

Figure 4. The magnetic field component variances normalized by $|B|^2$. The normalized variances within the high-speed stream proper (beyond the RS). are about equal to those in the trailing portion of the CIR. There also are enhanced variance values at and near the RS. The insert at the bottom give θ_{kB} values for Alfvénic waves within the CIR. 'l'he waves are generally found to be propagating at large angles to $\vec{B}_o$. The anisotropy factor for mirror mode growth is shown at the bottom of the insert. The only region that is unstable (R > 1.0) is at the RS. The remainder of the region between the IF and RS is marginally stable.

Figure 5. Some examples of mirror mode structures (1(J51 -1655111', 1700 UT, 1706-1709 UT). These arc sharp dips in |B| with no significant angular changes. The bottom panel is a hodogram of the wave between the dashed lines shown in the upper panel. The wave is left-hand elliptically polarized in the spacecraft frame.

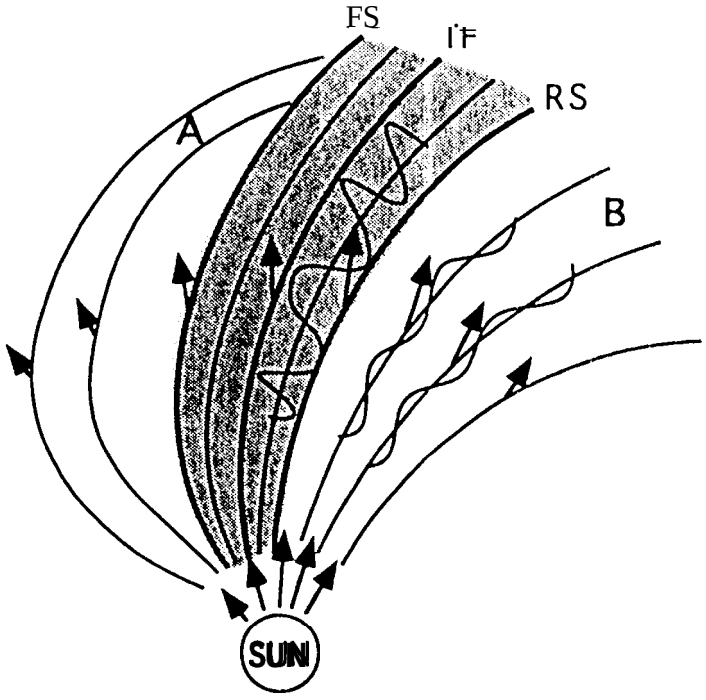

FIG. 1

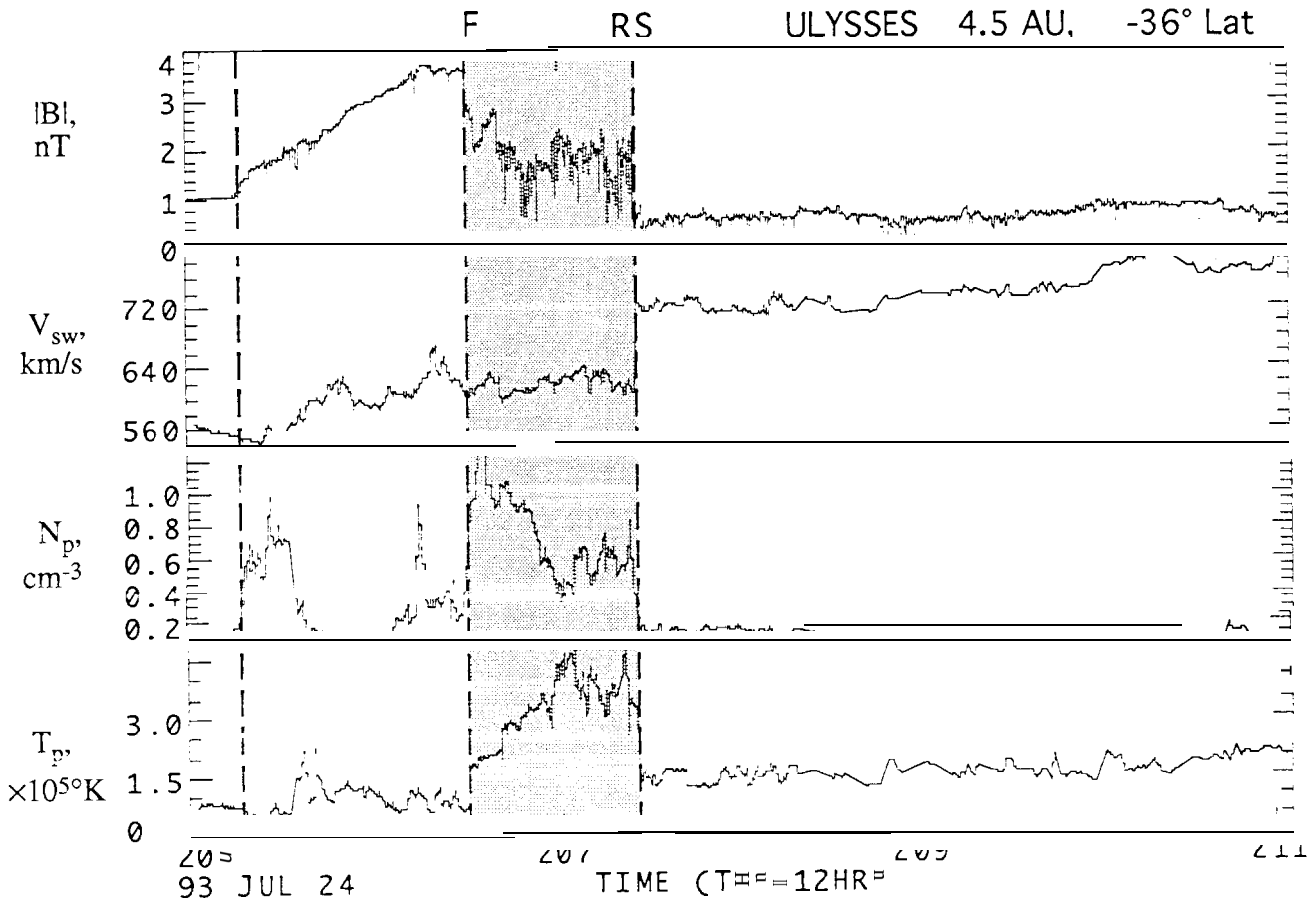
F
RS
ULYSSES 4.5 AU, -36° Lat
|B|, nT
4
3
2
1
0
V_{sw}, km/s
720
640
560
N_p, cm^{-3}
1.0
0.8
0.6
0.4
0.2
T_p, $\times 10^5$°K
3.0
1.5
0
93 JUL 24
TIME (T==12HR=

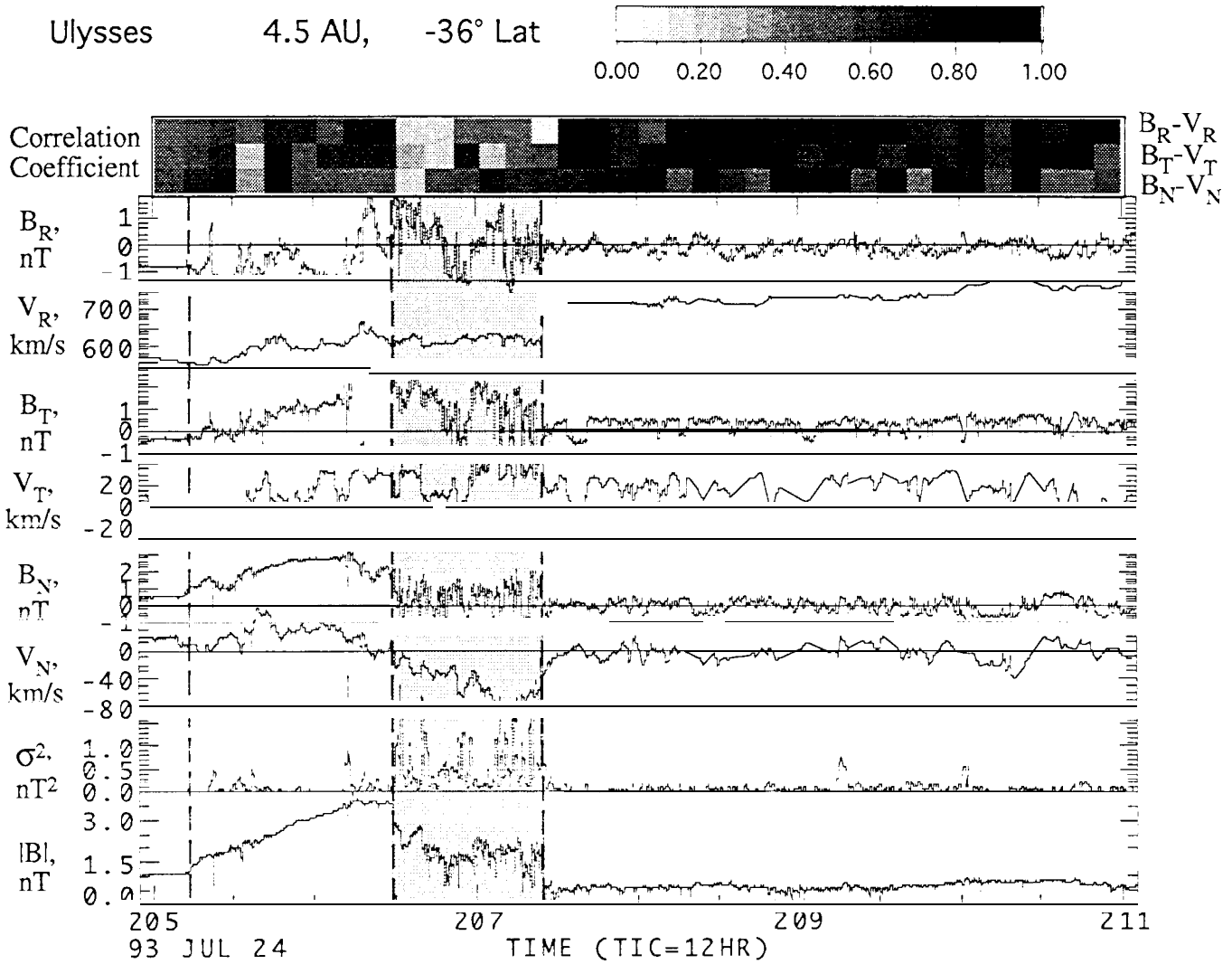
Ulysses
4.5 AU,
-36° Lat
0.00
0.20
0.40
0.60
0.80
1.00
Correlation Coefficient
B_R-V_R
B_T-V_T
B_N-V_N
B_R, nT
V_R, km/s
B_T, nT
V_T, km/s
B_N, nT
V_N, km/s
σ^2, nT^2
|B|, nT
205
207
209
211
93 JUL 24
TIME (TIC=12HR)

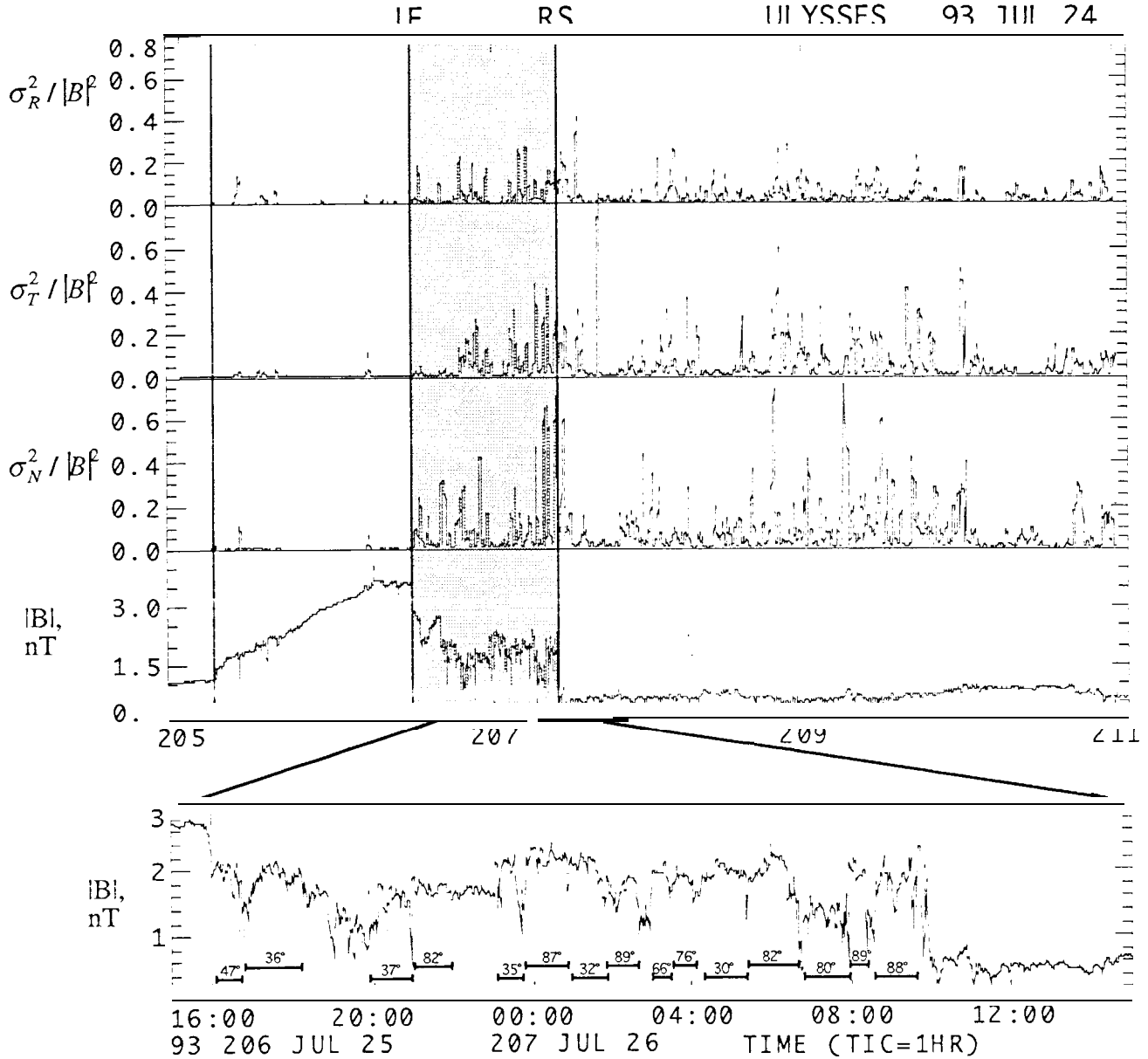
$\sigma_R^2 / |B|^2$
$\sigma_T^2 / |B|^2$
$\sigma_N^2 / |B|^2$
0.8
0.6
0.4
0.2
0.0
|B|, nT
3.0
1.5
0.
205
207
209
211
3
2
1
47°
36°
37°
82°
35°
87°
32°
89°
66°
76°
30°
82°
80°
89°
88°
16:00
20:00
00:00
04:00
08:00
12:00
93 206 JUL 25
207 JUL 26
TIME (TIC=1HR)

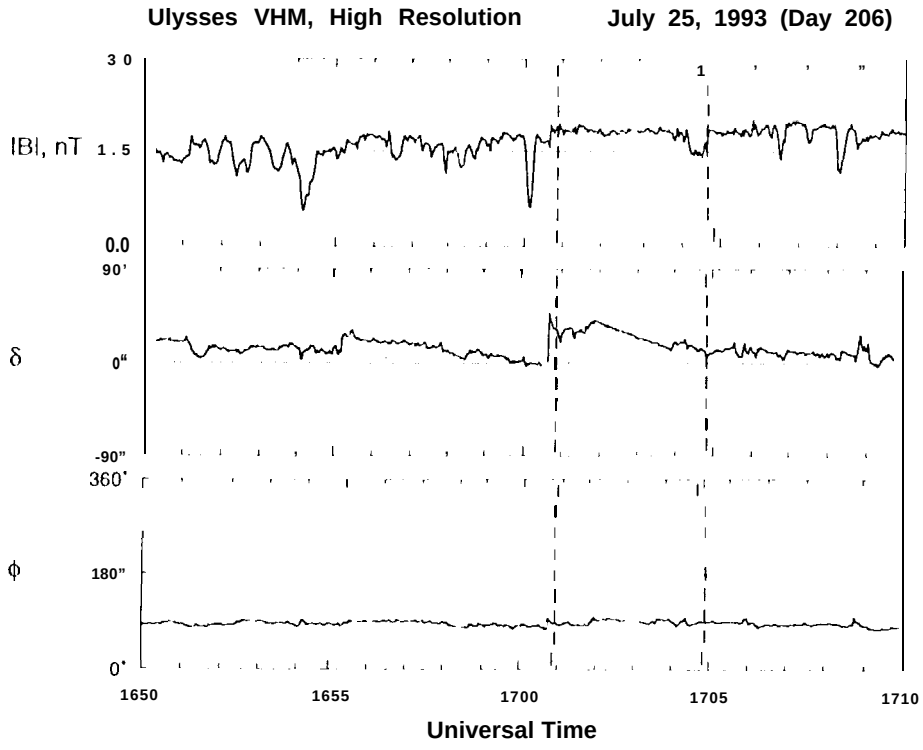
Ulysses VHM, High Resolution
July 25, 1993 (Day 206)
|B|, nT
δ
ϕ
30
1.5
0.0
90°
0°
-90°
360°
180°
0°
1650
1655
1700
1705
1710
Universal Time

a)

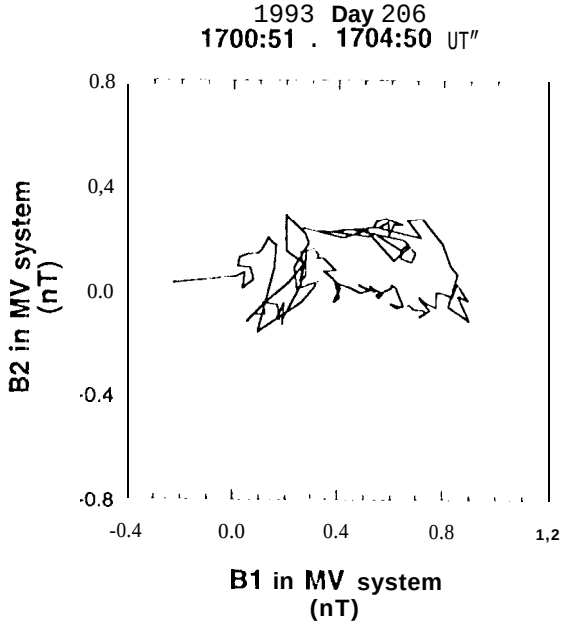
1993 Day 206
1700:51 . 1704:50 UT
B2 in MV system (nT)
0.8
0,4
0.0
-0.4
-0.8
-0.4
0.0
0.4
0.8
1,2
B1 in MV system (nT)

b)